JOURNAL OF MATERIALS SCIENCE 14 (1979) 535–540

Segregation in $Pb_{1-x}Sn_x$ Te during solidification by the Bridgman technique

V. FANO, R. PERGOLARI, L. ZANOTTI
Laboratorio MASPEC del C.N.R., Parma, Italy

The influence of the growth parameters on the concentration gradient of $Pb_{1-x}Sn_x$Te monocrystals grown by the vertical Bridgman technique is described. The concentration profiles of all three constituents (Pb, Sn, Te) have been analysed in ingots having different Pb–Sn ratios and grown under different conditions. The presumed role played by free convection in the Pb–Sn ratio is shown. Te was found to be constant in all ingots and not dependent upon the growth conditions.

1. Introduction

In $Pb_{1-x}Sn_x$Te monocrystals commonly synthesized by the vertical Bridgman technique, the parameters directly affecting the technological properties (for example the time dependence of the thermoelement figure of merit, the sink formation in non-radiative electron and hole recombination, nonplanarity in diffused p–n junctions for infra-red devices, the band-gap fixed by Pb–Sn stoichiometric ratio, etc.) depend upon the growth conditions. In these monocrystals two types of segregation are possible:

(a) a micro-segregation characterized by the presence of low-angle grain boundaries and inclusions which may vary in number along the crystal. This type of segregation can be limited by decreasing the growth velocity (V) and/or increasing the temperature gradient in the melt (G_1) along the growth axis. For a composition ratio metal:tellurium = 1:1 it was seen [1] that a low growth velocity such as 1 cm day^{-1} together with a temperature gradient of 10° C cm^{-1} invariably produced both inclusions and low-angle grain boundaries; (b) a normal segregation parallel to the solidification direction involving x value variation. This variation is dependent upon the temperature–composition phase diagram of the system. In [2] an example of a significant x variation along all of the ingot is shown. This type of segregation can be avoided if the steady state region of the diffusion-controlled distribution is formed. This allows the effective distribution coefficient (K_{eff}) to be constant.

When $V = 1$ cm day^{-1} and low G_1 were used, a significant part of the monocrystal presented a high degree of homogeneity in the Pb–Sn ratio, as reported by Calawa *et al.* [3], thus indicating that growth conditions in which the growth process occurs with mixing in the melt by diffusion alone, can be established. This possibility was tested by varying the growth parameters; in fact if a higher temperature gradient in the melt is used, micro-segregation would be limited without normal segregation alteration. This occurs if the interface curvature variation effects and convection mixing effects, resulting from the density gradient, do not appear. The K_{eff} value can be influenced by both of these effects.

In this work the concentration gradient of three elements (Pb, Sn, Te) along the growth axis is chemically analysed. Samples cut from ingots, grown by the vertical Bridgman technique, were used in these analyses and monocrystals with different starting Pb–Sn ratios were synthesized. The effects of different G_1/V values on the normal segregation were observed when either one or both of the parameters was changed. The experimental data are compared with the diffusion layer thickness value, δ, calculated for the different growth conditions; in fact, it is well known that δ depends upon the degree of mixing [4]. It was thus verified that during the solidification by the vertical Bridgman technique, the $Pb_{1-x}Sn_x$Te compositions are susceptible to free convection.

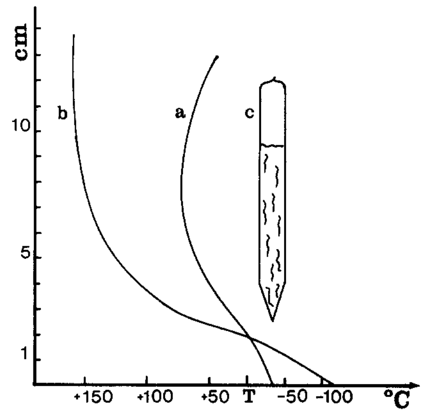

Figure 1 (a) and (b). Temperature profiles for growing crystals with the alloy compositions used. Curve a corresponds to temperature profile of 20° C cm^{-1} at the solid–liquid interface, curve b corresponds to a 60° C cm^{-1} profile. T is the melting temperature of the particular alloy compositions. (c) A schematic drawing of the starting position of the charges.

2. Experimental details

Starting elements 99.999% and further purified with oxygen (keeping them at melting point for a few hours in an H_2 flux) were used. The monocrystals were grown in quartz tubes after a direct synthesis of the polycrystals from the elements. Graphite coating of the quartz tubes was not necessary. The following G_1/V values were used: 2.4×10^3 °C min cm^{-2} (at crystallization front $G_1 = 20°$ C cm^{-1}, $V = 8.33 \times 10^{-3}$ cm min^{-1}), 7.2×10^3 °C min cm^{-2} (at crystallization front $G_1 = 60°$ C cm^{-1}, $V = 8.33 \times 10^{-3}$ cm min^{-1}), 1.2×10^4 °C min cm^{-2} (at crystallization front $G_1 = 20°$ C cm^{-1}, $V = 1.67 \times 10^{-3}$ cm min^{-1}), 3.6×10^4 °C min cm^{-2} (at crystallization front $G_1 = 60°$ C cm^{-1}, $V = 1.67 \times 10^{-3}$ cm min^{-1}). In Fig. 1, the two temperature gradients along the quartz tube are reported.

Average monocrystal ingot dimensions were 1.3 cm wide and 6 cm high, and the first-to-freeze 1.5 cm height had a conical shape. The samples (~ 100 mg) were sliced perpendicular to the ingot growth axis and then underwent chemical analysis following the procedure described in [5], the experimental error being ± 1%. The Pb, Sn and Te were determined in a sample solution by successively adding appropriate and selective reagents. For Pb these concentration profiles were in agreement with those found by X-ray fluorescence as seen in [6]. The Hall constant (R_H) and Hall mobility $\mu = R_H\,\sigma$ (σ is the electrical conductivity) were also measured. Cross modulation of both the sample current (at a frequency of 84 Hz) and the magnetic field (1500 G at a frequency of 36 Hz) were used for the simultaneous σ and R_H measurements. The Hall voltage was detected at the sum frequency (120 Hz), thus interference from spurious effects was eliminated. The results of these measurements were fairly similar to those reported by Calawa *et al.* [3] and Wagner *et al.* [7]. For the same chemical composition, the values were frequently different. In Table I, hole carrier concentration (p) and Hall mobility values at 300 K and 77 K are reported. These measurements refer to the same samples, cut from the ingot zone having a lower degree of compositional gradient (see below) and then successively symmetrically thinned. These measurements (electrical, geometrical and Hall voltage) had an estimated precision of ± 5% or better. Therefore, for the thinned samples, the p and μ variations were greater than experimental error and thus this

TABLE I The carrier concentration and Hall mobility in some samples (a, b, c). For every sample the measurements have been made at different thicknesses.

Sample composition	Thickness of samples (a, b, c) (mm)		Carrier concentration ($\times 10^{19}$ cm^{-3})		Hall mobility (cm^2 V^{-1} sec^{-1})	
			at 77 K	at 300 K	at 77 K	at 300 K
$Pb_{0.91}Sn_{0.19}Te$	1.31	a	1.0	3.3	1100	650
	0.92		1.0	2.8	1075	720
	0.50		3.5	7.0	830	510
$Pb_{0.75}Sn_{0.25}Te$	1.20	b	2.8	5.2	580	340
	0.85		2.8	4.3	560	400
	0.65		4.2	6.5	280	272
$Pb_{0.7}Sn_{0.3}Te$	1.25	c	7.2	8.1	460	445
	0.85		7.0	79	280	215
	0.65		7.1	8.9	365	320

means that these properties are very dependent upon first-type defect concentration fluctuation. For this reason, electrical measurement data for the stoichiometric calculation of as-grown crystals were not employed in this work.

The liquidus compositions for the K_{eff} calculations were determined from the weight of the elements.

3. Results and discussion

3.1. Effect of convection

Fig. 2 shows x variations in ingots with different starting compositions ($1-x=0.83$ and 0.60, respectively; Te = 1 is maintained throughout) grown with two different G_1/V values (2.4×10^3 and 3.6×10^4 °C min cm^{-2}). For $0.83 \leqslant x \leqslant 0.60$, the curve behaviours were similar when the same G_1/V values were used. Curves a and b of Fig. 2, where $G_1/V = 2.4 \times 10^3$ °C min cm^{-2} growth conditions were used, showed a steady-state region in the first-to-freeze solid in which Pb and Sn content were practically constant. The K_{eff} values of both starting compositions calculated in this region (about mid-height of the conical part of the single crystal) are in agreement with phase diagram data reported by Calawa *et al.* [3] and Wagner *et al.* [8] but are different from those reported by Abrikosov *et al.* [9]. According to the $\mathrm{Pb}_{1-x}\mathrm{Sn}_x\mathrm{Te}$ phase diagram (the liquidus and solidus lines of the PbTe–SnTe pseudobinary system form a lens-shaped diagram exhibiting complete solid solubility) for any starting element composition with $x \neq 0$ or 1, there must be a normal segregation of the solute i.e. of Sn ($K_{\mathrm{eff}}^{\mathrm{Sn}} < 1$) or of Pb ($K_{\mathrm{eff}}^{\mathrm{Pb}} > 1$). This normal tin (lead) segregation can be represented by a single curve, in which the Sn(Pb) concentration within the ingot is related to the distance from the start of crystallization. It is well known that the form of this curve depends upon the equilibrium distribution coefficient, the growth velocity and the amount of mixing of the melt. If the crystal grows from the melt free of mixing, the transport of the solute being entirely by diffusion, a steady-state condition may be reached in which the solute concentration is constant (K_{eff} = constant). Under these conditions, $\delta > D/V$ can be considered where D/V is the diffusion distance. Thus at first sight it would seem that sections of curves a and b of Fig. 2, where x is practically constant, may be connected with the growth process under $\delta > D/V$ conditions. This means that even if there is convection, the δ thickness is not affected by it; this convection being caused by Sn rejection within the melt. In fact, the enrichment by Sn decreases the $\mathrm{Pb}_{1-x}\mathrm{Sn}_x\mathrm{Te}$ melt density. Therefore, the mixing by convection is due to the difference in the constituent density near the interface (generally the difference in density caused by the temperature gradient is neglected in the vertical Bridgman

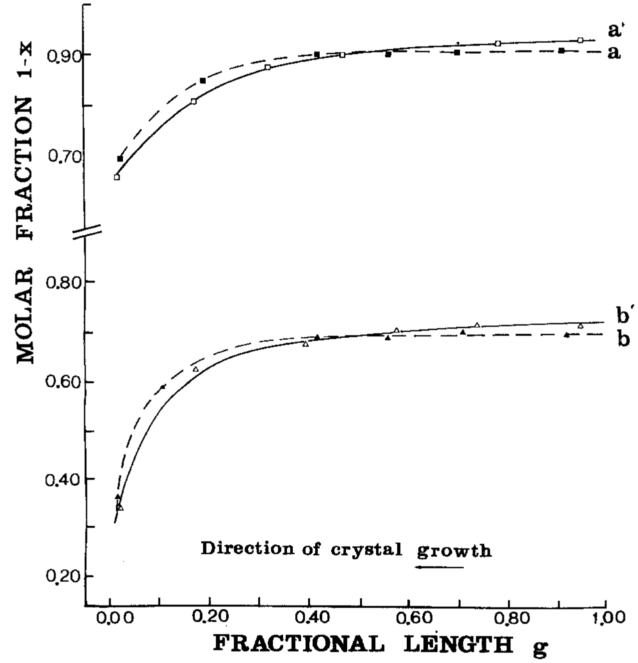

Figure 2 The $1-x$ coefficient in $\mathrm{Pb}_{1-x}\mathrm{Sn}_x\mathrm{Te}$ ingots plotted as a functions of the fractional length $g = l/L$ (l is the solidified fraction, L is the total length of the ingots. Curves a and b (■ and ▲) refer to growth conditions $G_1/V = 2.4 \times 10^3$ °C min cm^{-2}; curves a′ and b′ (□ and △) refer to growth condtions $G_1/V = 3.6 \times 10^4$ °C min cm^{-2}. The starting $1-x$ values were as follows; for a and a′ $1-x = 0.83$, for b and b′ $1-x = 0.60$.

TABLE II The effective distribution coefficients of lead and tin ($K_{\text{eff}}^{\text{Pb}}, K_{\text{eff}}^{\text{Sn}}$), and the diffusion layer thickness (δ) for different melt compositions at different growth conditions

Melt composition	$K_{\text{eff}}^{\text{Pb}}$		$K_{\text{eff}}^{\text{Sn}}$	
	$G_1 = 20°$ C cm^{-1}	$G_1 = 60°$ C cm^{-1}	$G_1 = 20°$ C cm^{-1}	$G_1 = 60°$ C cm^{-1}
$Pb_{0.83}Sn_{0.17}Te$	1.10	1.12	0.53	0.41
$Pb_{0.70}Sn_{0.30}Te$	1.08	1.13	0.82	0.70
$Pb_{0.60}Sn_{0.40}Te$	1.17	1.22	0.74	0.67

Melt composition	δ (cm)	
	$G_1 = 20°$ C cm^{-1} $V = 1.66 \times 10^{-3}$ cm min^{-1}	$G_1 = 60°$ C cm^{-1} $V = 8.33 \times 10^{-3}$ cm min^{-1}
$Pb_{0.83}Sn_{0.17}Te$	2.2×10^{-2}	1.1×10^{-2}
$Pb_{0.70}Sn_{0.30}Te$	2.3×10^{-2}	1.1×10^{-2}
$Pb_{0.60}Sn_{0.40}Te$	2.4×10^{-2}	1.2×10^{-2}

technique). For a better understanding of the role played by convection it would be interesting to analyse the compositional shape of a few millimetres in the first-to-freeze crystal. In this way some information about the initial transient region could be obtained according to Tiller *et al.* [10]. Unfortunately, this is not possible since the growth by the vertical Bridgman technique of the first few millimetres of the crystal is dominated by other factors which cause an unexpected tin enrichment of this zone [11]. On the other hand, by increasing the G_1/V value (3.6×10^4 °C min cm^{-2}) the growth of crystals having the same starting composition brings about a change in K_{eff} which is calculated at approximately mid-height of the conical part of the single crystal (see Table II). Thus the high degree of Pb–Sn ratio homogeneity no longer exists even though the ingots present an increase in crystal grain sizes which at times reach tube section dimensions. In this case, it is clear that growth takes place under $\delta < D/V$ conditions and, therefore, the solute transport in the melt can be influenced by the free convection. In fact, if it were not experimentally demonstrated, the apparent δ diminution with respect of D/V attributed only to the V diminution could result in oversimplification. The role of the mixing will be verified experimentally together with δ calculation.

3.2. Effect of interface shape

In addition to mixing by convection, another effect could affect the compositional variation along the ingot if the temperature in the upper zone of the Bridgman system is increased. Neglecting capillarity, the use of the gradient in Fig. 1b leads to an interface curvature variation which becomes more concave (less convex). As a result of this curvature variation there could be a higher solute (Sn) content in the melt adjacent to the interface with a G_1 increase. Consequently, the composition of the first-to-freeze solid must be richer in Sn than that of the lower G_1 ($V =$ const.). If this does not occur, it means that the effect of

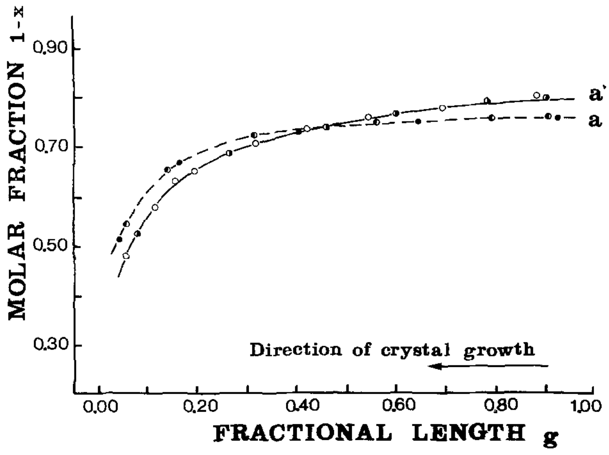

Figure 3 The $1-x$ coefficient in ingots with $Pb_{0.7}Sn_{0.3}Te$ starting compositions as a function of the fractional length $g = l/L$. Curve a refers to growth conditions $G_1/V = 2.4 \times 10^{3}$° C min cm^{-2} (●) and $G_1/V = 1.2 \times 10^{4}$° C min cm^{-2} (○); curve a′ refers to growth conditions $G_1/V = 7.2 \times 10^3$ ° C min cm^{-2} (○) and $G_1/V = 3.6 \times 10^4$ ° C min cm^{-2} (◑).

interface curvature variation is negligible. On the contrary, if the Pb content increases in the first-to-freeze solid, this effect can be attributed to the appearance of free convection, and use of the gradient in Fig. 1b could limit the negative effects of supercooling. As will be seen in the next section, the effect of the interface shape on the compositional variation can be excluded.

3.3. Effect of growth velocity and thermal gradient.

Fig. 3 shows results obtained from ingots with starting compositions corresponding to $Pb_{0.7}Sn_{0.3}Te$. Curve a (solidus circles) refers to an ingot having the same growth velocity as those in curves a and b of Fig. 2. As usual, $G_1/V = 2.4 \times 10^3$ °C min cm^{-2} produces a large first-to-freeze solid with an almost constant x. This situation does not vary when a lower velocity is used, i.e. for $G_1/V = 1.2 \times 10^4$ °C min cm^{-2} (Fig. 3 curve a ◑). The open circles of curve a′ of Fig. 3 refer to an ingot grown at a higher thermal gradient, i.e. when $G_1/V = 8.2 \times 10^3$ °C min cm^{-2} is applied. A worsening in the Pb–Sn ratio homogeneity is evident and is comparable with growth with reduced velocity, i.e. $G_1/V = 3.6 \times 10^4$ °C min cm^{-2} is applied (Fig. 3a′ ◑); the concentration gradient is, of course, higher in the last-to-freeze solid. Furthermore, the first-to-freeze solid is poorer in Sn content, thus the probable shape variation of the interface does not appreciably affect the normal segregation. Therefore, it can be assumed that a significant contribution to the Pb–Sn ratio along the growth axis depends upon the G_1 value. Inclusions, smaller but similar to those reported in [1], have been observed in these ingots. These defects are usually attributed to constitutional supercooling effect. The use of the maximum G_1/V value (3.6×10^4 °C min cm^{-2}) while producing a compositional gradient in the first-to-freeze part does not guarantee inclusion-free monocrystals. No attempt to synthesize inclusion-free ingots, by increasing the G_1, was attempted, because it would have caused even more of a compositional gradient along the growth axis. On the other hand, a further growth velocity decrease, up to 3 cm day^{-1}, as in [1], combined with a low G_1 value (for preventing normal segregation $G_1 \leqslant 20°$ C cm^{-1}) does not lead to a G_1/V increase and, consequently, constitutionally supercooled structures are not eliminated. In practice, depending upon how the material will be used, a compromise between G_1 and V must be made.

3.4. δ calculation

We are now in a position to estimate the δ value both for the various compositions and also for the different growth conditions and to compare it with the D/V. Approximating our growth system to that of the liquid zone in a vertical tube moving down, we have (using the same symbols and following the methods in [12])

$$\delta = \frac{B_1 a}{|B_2|\,(a/l)^{0.44}(\rho V/D)^{0.26}},$$

where B_1 is a constant, whose value for the vertical Bridgman growth method depends on the sign of the difference between the bulk melt density and the melt at the solid–liquid interface; B_2 is dependent on some dimensionless parameter (Prandtl, Schmidt and Grashof numbers); a is the radius of the quartz tube; l is the length of the melted zone; ρ is the density of the melt. The inconvenience of using this calculation is that many of the physical parameters of the various compositions, density, viscosity, etc., are unknown. However, these parameters can be calculated from the values of the pure components (PbTe and SnTe) and from the x composition, since the PbTe–SnTe pseudo-binary system can be approximated to quasi-ideal binary solution [8, 9]. Even if the solidus and liquidus lines, as described by different authors, do not have the same values, these deviations do not affect our conclusions. The viscosity and density values of the end members (PbTe and SnTe) have been taken from [13]. The specific heat values are between 0.15 J g^{-1} for $1 - x = 0.83$ and 0.16 J g^{-1} for $1 - x = 0.6$ [14]. A diffusion constant of $D = 5 \times 10^{-5}$ cm^2 sec^{-1} and a thermal conductivity of 0.055 W° C^{-1} cm^{-1} were maintained for all compostions [15]. The length of the liquid zone was kept at 6 cm, at the point at which growth within the cylindrical zone of the quartz tube was initiated.

The δ values are typical of those partial melt mixing by free convection (1×10^{-2} cm $< \delta <$ 2.5×10^{-2} cm) as seen in Table II. They are about 1 order of magnitude lower than D/V ($D/V =$ 0.36 cm for $V = 8.33 \times 10^{-3}$ cm min^{-1}; $D/V =$ 1.8 cm for $V = 1.67 \times 10^{-3}$ cm min^{-1}). Therefore, it cannot be stated that the monocrystal composition is dominated by the diffusion process. In

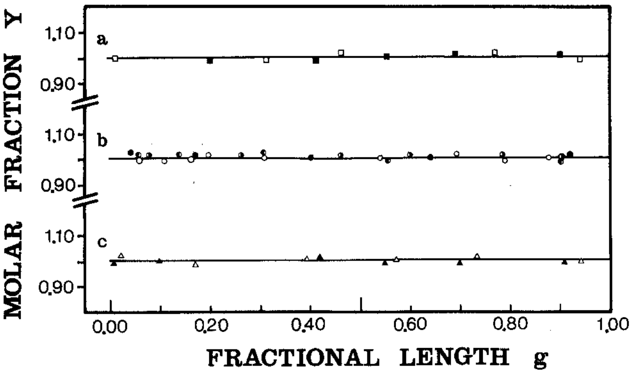

Figure 4 The y coefficient in $(Pb_{1-x}Sn_x)Te_y$ ingots plotted as a function of the fractional length $g = l/L$. The starting y values were constant and equal to 1. The symbols have the same significance as in Figs. 2 and 3.

fact, a very high velocity must be used (tens of centimetres per second) so that $\delta \sim D/V$. A velocity of this order of magnitude brings about the formation of polycrystal ingots. Certainly the apparent uniformity of the composition in the first-to-freeze solid at $G_1 = 20°$ C cm is favoured by the geometry of the quartz container. Moreover, as can be seen in the calculation, the increase of temperature gradient from 20 to 60° C cm^{-1} is not enough to bring about such a considerable δ variation as in $\delta \sim D/V$. Nevertheless, because of the Soret effect the temperature gradient could also effect the Sn transport in the melt and, consequently, also the value of K_{eff}. Thus the contribution of this effect cannot be excluded.

Finally, in Fig. 4, Te content along the growth axis is shown. As can be seen, the tellurium concentration is constant within experimental error independent of the applied G_1/V values.

Acknowledgement

Thanks are due to Mrs M. Battaglioli for her assistance in the synthesis of the crystals.

References

1. J. F. BUTLER and T. C. HARMAN, *J. Electrochem. Soc.* **116** (1969) 260.
2. D. MATEIKA, *J. Crystal Growth* **9** (1971) 249.
3. A. R. CALAWA, T. C. HARMAN, M. FINN and P. YOUTZ, *Trans. Met. Soc. AIME* **242** (1968) 374.
4. W. G. PFANN, "Zone Melting" (Wiley, New York, 1958) p. 13.
5. V. FANO and L. ZANOTTI, *Microchem. J.* **18** (1973) 1.
6. V. FANO, C. GHEZZI and L. ZANOTTI, *Appl. Spectros.* **30** (1976) 359.
7. J. W. WAGNER, A. G. THOMPSON and R. K. WILLARDSON, *J. Appl. Phys.* **42** (1971) 2515.
8. J. W. WAGNER and R. K. WILLARDSON, *Trans. Met. Soc. AIME* **242** (1968) 366.
9. N. KH. ABRIKOSOV, K. A. DYUL'DINA and T. A. DANYLIAN, *Zh. Neorgan. Khim* **3** (1958) 1632.
10. W. A. TILLER, K. A. JACKSON, J. W. RUTTER and B. CHALMERS *Acta Met.* **1** (1953) 428.
11. V. FANO, and C. GHEZZI, unpublished work.
12. J. C. BRICE, in "The growth of Crystals from Liquids", edited by E. P. Wohlfarth (North Holland, Amsterdam, 1973) p. 135.
13. V. M. GLAZOV, S. N. CHIDZEVSKAIA and N. H. GLAGOLIEVA, in "Djidkie poluprovodniki" (Nauka, Moscow, 1967).
14. P. AIGRAIN and M. BALKANSKI, "Constantes sélectionées relatives aux semiconducteurs" (Pergamon Press, Oxford, 1961).
15. V. I. FEDOROV and V. I. MACHUEV, *Sov. Phys. Solid State* **11** (1969) 1116.

Received 28 February and accepted 20 July 1978.